SCIENTIFIC PAPER
Published: October 24, 2025
https://doi.org/10.13167/2025.31.9

Comparative study on predicting the compressive strength of oven-cured fly ash and slag-based geopolymer concrete using soft computing techniques

Pramod Kumar[1], Sanjay Sharma[2] and Bheem Pratap[1]✉

[1] *Graphic Era Deemed to be University, Department of Civil Engineering, 248002, Dehradun, India*

[2] *Mohan Babu University, Faculty, Department of Civil Engineering, 517102, Tirupati, India*

Corresponding author:
Bheem Pratap

Received:
September 4, 2024

Revised:
April 5, 2025

Accepted:
July 11, 2025

Published:
October 24, 2025

Citation:
Kumar, P.; Sharma, S.; Pratap, B. Comparative study on predicting the compressive strength of oven-cured fly ash and slag-based geopolymer concrete using soft computing techniques. *Advances in Civil and Architectural Engineering,* 2025, 16 (31), pp. 146-164. https://doi.org/10.13167/2025.31.9

ADVANCES IN CIVIL AND ARCHITECTURAL ENGINEERING (ISSN 2975-3848)

Faculty of Civil Engineering and Architecture Osijek
Josip Juraj Strossmayer University of Osijek
Vladimira Preloga 3
31000 Osijek
CROATIA

Abstract:
Sustainable concrete is created using waste materials and contributes to environmental conservation. In this study, fly ash and slag were key ingredients for this sustainable concrete. The focus was on constructing a predictive model using various input variables. To achieve this, machine learning techniques were employed: random forest (RF), support vector machine (SVM), and long short-term memory (LSTM). These algorithms were used to predict the properties of structural concrete produced from fly ash and slag. The predictive model was precisely trained and tested using experimental data. The assessment of model performance involved a comparative analysis based on two metrics: the coefficient of determination score and root mean square error. The coefficient of determination values for the RF, SVM, and LSTM were 0,8439; 0,8668; and 0,8694; respectively. The root mean square error values were 4,0318; 3,9692; and 3,6921 for RF, SVM, and LSTM, respectively. The results of this study demonstrate that the LSTM model outperformed both the RF and SVM models. This suggests that the LSTM algorithm is particularly suitable for capturing complex patterns and relationships within the data, making it well-suited for predicting the properties of sustainable concrete based on fly ash and slag.

Keywords:
fly ash; granulated blast-furnace slag; structural concrete; machine learning; compressive strength

1 Introduction

Geopolymers, also known as alkali-activated binders, represent a class of cementitious materials formed by the reaction between a solid aluminosilicate material (such as pulverised fly ash, granulated blast-furnace slag, clay, or volcanic rock) and an alkali activator. This chemical process, known as geopolymerisation, leads to the formation of gel phases and is similar to the formation of zeolites, which are part of the aluminosilicate group. Although geopolymers and zeolites have some chemical similarities, they exhibit distinct differences in crystallinity and amorphous nature. The concept of geopolymers has been under investigation since the 1970s, and has garnered significant attention from researchers. Consequently, numerous international patents have been associated with this technology, which has been applied in various commercial engineering projects. Geopolymers have shown promising mechanical and thermal properties, as highlighted by Juenger et al. (2011) [1], making them potential substitutes for traditional Portland cement, particularly in low-risk and specialised applications. Increasing interest in sustainable and environmentally friendly construction materials has fuelled the research and development of geopolymers [2-6].

Geopolymer concrete (GPC) is a promising alternative to conventional concrete owing to its low carbon footprint [7] and high durability. A critical component of GPCs is fly ash, a byproduct of coal-fired power plants that serves as a binder. However, fly ash-based GPC often suffers from low early-age strengths, which is a significant drawback for practical applications. Researchers have explored the use of a combination of fly ash and ground granulated blast furnace slag (GGBFS) [8] in GPC. GGBFS is a byproduct of the ironmaking industry and has a relatively high calcium content. When added to fly ash-based GPC, GGBFS significantly enhances the characteristics of the resulting mixture [9-12]. Several studies have focused on GPCs containing both fly ash and GGBFS, but it is worth noting that most previous studies have mainly concentrated on GPCs that solely utilised fly ash as the binder. This highlights the novelty and potential benefits of investigating GPCs using a combination of fly ash and GGBFS [13]. Nath and Sarker (2014) [14] demonstrated that adding GGBFS to fly ash-based GPCs helped achieve compressive strengths comparable to those of conventional concrete. This result is significant because it indicates that GPCs with improved mechanical properties can be produced by incorporating GGBFS into the formulation. Moreover, the specific composition of the fly ash/GGBFS blend plays a crucial role in determining the compressive and flexural strengths of the geopolymers, as indicated by Marjanovic et al. (2015) [15]. This underlines the importance of careful optimisation and mixture design when creating GPCs that combine fly ash and GGBFS. GPC is an environmentally friendly alternative to conventional cement-based concrete, and GGBFS is one of the most common waste materials used in its production. Even when used in small quantities, such as 4%, GGBFS enhanced the strength of the fly ash-based GPC [16]. However, the degree of improvement depends on various factors, including the type and strength of the activating solution and the proportion of GGBFS and fly ash in the mixture [14; 16]. A previous study suggested that curing conditions also play a crucial role in the performance of geopolymer concrete. When the precursor materials have a high calcium oxide (CaO) content and are cured at room temperature, the resulting GPC exhibits several advantages. They exhibit increased strength, faster setting times, and improved mechanical properties [14]. The presence of CaO in the precursor materials promotes the formation of stable and strong chemical bonds during the geopolymerisation process, leading to enhancements in the final concrete product.

In terms of the chemical composition, some geopolymers can be categorised as zeolites. Zeolites are crystalline aluminosilicate minerals with well-defined structures [17]. However, it is important to note that the X-ray diffraction (XRD) patterns of geopolymers differ significantly from those of zeolites. Although zeolites exhibit well-crystallised structures under XRD, geopolymers are amorphous and exhibit poor crystallinity when analysed using XRD [18]. The lack of long-range order in the atomic arrangement is a fundamental distinction between the geopolymers and zeolites. The unique properties of geopolymers stem from their chemical composition and geopolymerisation process. When an aluminosilicate material [19; 20] is

mixed with an alkaline activator, such as sodium hydroxide or potassium hydroxide, it forms a three-dimensional polymeric network. This network is responsible for the strength and binding properties of the geopolymers. The resulting material can be used as a durable binder in various construction applications.

Alkaline solutions prepared using a combination of sodium hydroxide (NaOH) and sodium silicate (Na_2SiO_3) are suitable alkaline activators for preparing GPC. GPC is an innovative and eco-friendly alternative to traditional Portland cement-based concrete. It is formed by the reaction of aluminosilicate materials, such as fly ash and GGBFS, with alkaline activators. The choice of alkaline activators, specifically NaOH and Na2SiO3, is critical because it directly affects the performance and properties of GPC. Various studies have established that any change in the proportions of binders (fly ash and GGBFS), molarity of the NaOH solution, ratio of Na_2SiO_3 to NaOH solution, and curing temperature has a significant influence on the compressive strength of concrete [13; 21; 22]. The proportions of fly ash and GGBFS as binders in GPC significantly affects the overall performance and strength of the concrete. Different combinations of these materials yield varying results. Therefore, it is essential to optimise the binder content to achieve the desired strength and durability. The molarity of the NaOH solution used as an alkaline activator is crucial for geopolymerisation. Previous studies have suggested that a NaOH solution with a molarity range of 8-12M effectively achieves the required compressive strength for GPC. The Na_2SiO_3 to NaOH ratio is another critical parameter for controlling the geopolymerisation reaction. A recommended ratio of 2,5 has been proposed in some studies to obtain desirable properties in the resulting concrete [20; 23].

Empirical regression methods appear to be more appropriate than conventional experimental approaches for evaluating the compressive load-carrying ability of concrete. With advances in artificial intelligence, the use of machine learning techniques to estimate the compressive strength of concrete has become increasingly popular and practical. Machine learning techniques, including decision trees, RF, SVM, and artificial neural networks, have been extensively used to estimate the compressive strength of concrete. The research findings revealed that machine learning performed well in the regression prediction of the concrete strength. Nevertheless, most of the algorithms used in this research are conventional machine learning algorithms with little predictive power. Model tweaking is necessary to obtain the correct model parameters for improved prediction performance; however, this process is also difficult [24]. Investigating a deep learning model with superior prediction performance is better than that of traditional machine learning techniques [25-26]. For both long- and short-term forecasting, LSTM models have proven to be superior to other models; however, the LSTM model has issues with model complexity and lengthy training. Therefore, appropriate data processing can improve the learning impact of the LSTM models. The accuracy of LSTM forecasting was achieved by a multiple-variable LSTM algorithm, performing dimensionality reduction on the original data using the wavelet noise reduction method, and then reconstructing preselected input data using chaos analysis and the classification forecast tree method [27]. Because it is difficult to define shear strength using large-scale strength testing, machine learning approaches based on support vector machine (SVM) and random forest (RF) models have been suggested.

This study aims to analyse the experimental results and develop machine learning (ML) models to explore the compressive strength of structural GPC made from fly ash and slag using the oven-curing technique. Three ML algorithms were considered in this study: RF, SVM, and LSTM. Each algorithm has unique characteristics and capabilities, making it suitable for predicting the concrete strength. To conduct a comparative study, we first preprocessed the dataset, including data cleaning and feature engineering. The data were then entered into the training and testing sets to evaluate the performance of each ML algorithm. The algorithms were trained on the training set, where they learned the patterns and relationships in the data, and then tested on the testing set to measure their predictive accuracy.

2 Methodology

2.1 Materials and methods

GGBFS, a cementitious material widely used in the construction industry, is derived from the iron and steel sector. Its pozzolanic and hydraulic properties were estimated from the Jojobera Power Plant in Jamshedpur, Jharkhand (India), and fly ash was collected from M/s. Usha Martin, Jamshedpur, Jharkhand, India. The precursor used in this study was GGBFS with a specific gravity of 2,78. X-ray fluorescence (XRF) for fly ash and GGBFS are listed in Table 1. Before being used in the experiment, raw GGBFS and fly ash were both oven-dried at 105 °C and sieved through a 75-micron mesh. Because NaOH is exothermic, it was prepared 24 h before testing. The mixture was stirred for 30 min using a magnetic stirrer to ensure complete dissolution of the NaOH pellets. Sodium hydroxide (98 % pure) and sodium silicate (1,57 specific gravity, Na_2O = 19,65 %, H_2O = 48,15 %, and SiO_2 = 32,20) were employed. A fine aggregate with a maximum size of 4,75 mm and a specific gravity of 2,67 was found in the Kharkai River, which complies with zone II of IS 383-1970 [23]. Use was made of coarse aggregate with a specific gravity of 2,74 and a maximum size of 20 mm.

Table 1. XRF results of GGBS and fly ash

Oxides content (% wt./wt.)	**Fly ash**	**GGBS**
Al_2O_3	28,57	15,87
SiO_2	45,85	33,64
CaO	7,45	30,84
Fe_2O_3	4,72	12,63
Na_2O	14,71	0,56
SO_3	0,34	0,41
P_2O_5	1,52	---

2.2 Mix design

The concentration of NaOH solution plays a crucial role in the production of geopolymer concrete. A sodium hydroxide strength of 12M was selected for this process. Molarity measures the concentration of a solute (in this case, NaOH) in a solution, indicating the number of moles of solute dissolved per litre of the solution. A higher molarity of NaOH enhances the activation of the geopolymer reaction, resulting in a stronger and more durable material. The alkaline activator solution-to-binder ratio was set at 0,50. This is the ratio of the alkaline activator solution (NaOH) to the binder material. Through meticulous preliminary trials, it was determined that this ratio offers optimal results for the geopolymerisation process, leading to desirable mechanical properties and overall performance of the final geopolymer product. The synthesis of geopolymer concrete involves the use of two key binder materials: GGBFS and fly ash. The quantities of GGBFS and fly ash used in the geopolymer formulations were within specified ranges. For GGBFS, the range was 108-225 kg/m^3, and for fly ash, the range was 180-315 kg/m^3. These ranges provide flexibility in formulation, allowing adjustments to achieve the desired properties and performance characteristics. Table 2 provides a breakdown of the design mix proportions for geopolymer concrete development, and shows how the combination of GGBFS and fly ash contributes to the composition of the final product.

For compressive strength testing, samples were created using moulds with dimensions of 150 × 150 × 150 mm. This standard size ensured uniformity and comparability of the testing results. During the casting process, the specimens were vibrated to eliminate trapped air, which could otherwise create voids and weaken them. After casting, the specimens underwent heat treatment and were exposed to 65 °C for 24 h. This elevated temperature accelerates geopolymerisation, a chemical reaction that significantly strengthens the material. After accelerated curing, the specimens were allowed to cool to room temperature. They were then stored at room temperature until testing or for approximately 28.

Table 2. Mix design of the geopolymer concrete

Concrete Ingredients	**Quantity** (kg/m^3)
GGBFS	108,00-225,00
fly ash	180,00-315,00
coarse aggregate	949,80-1090,80
fine aggregate	677,93-810,60
alkaline	162,00-270,00

2.3 Database

Research on concrete composed of fly ash and GGBS represents a noteworthy advancement in the field of building materials. Anaconda-based Python programming was used to obtain the experimental results. One output parameter related to the compressive strength of concrete was included in the database, along with nine input parameters that were part of the experimental program conducted in this study. Anaconda is a widely used open-source platform that provides extensive tools and packages specifically designed for Python data analysis and scientific computing. Its inclusion in this study underscores the significance of leveraging sophisticated data analysis techniques to comprehend the behaviour of concrete made with fly ash and GGBFS and to optimise its properties. A data-driven approach provides valuable insights into the properties of concrete based on fly ash-GGBFS. As a crucial concrete attribute, compressive strength was selected as an important output value. Five input parameters, namely fly ash, GGBFS, coarse aggregate (CA), fine aggregate (FA), and alkali solution, were selected for the investigation, which significantly influenced the compressive strength of the concrete. One of the primary advantages of using fly ash and GGBFS in concrete is their potential to enhance the overall strength and durability of the material. Fly ash, a byproduct of coal combustion, and GGBFS are considered supplementary cementitious materials. Incorporating these materials into concrete reduces waste and enhances the long-term performance. Therefore, to appreciate the potential of fly ash-GGBFS-based concrete, it is essential to understand the link between these input parameters and the final compressive strength. The analysis utilised a dataset comprising 120 data points, each representing a unique observation. The dataset contains several variables, and Table 3 provides essential information about these variables. This table lists the maximum and minimum values recorded among the 120 data points for each variable. The maximum value represents the highest observed value for that variable, whereas the minimum value represents the lowest value. Analysing the range of values for each variable is crucial for understanding the spread and distribution of data in the dataset. This information allows researchers to gain insight into the variability of the dataset and identify potential outliers or extreme values.

Table 3. Descriptive statistics

	Fly Ash	**GGBS**	**CA**	**FA**	**Alk.**	**CS_C**
count	120,00	120,00	120,00	120,00	120,00	120,00
mean	243,00	162,00	1037,14	766,13	212,63	49,85
std.	37,52	35,23	53,49	36,03	27,36	10,92
min.	180,00	108,00	949,80	677,93	162,00	26,89
25 %	215,00	129,00	966,00	753,75	192,63	42,30
50 %	243,00	162,00	1058,41	768,73	212,25	52,99
75 %	270,00	190,00	1080,27	797,00	231,75	57,82
max.	315,00	225,00	1090,80	810,60	270,00	65,26

The input and output attributes were built into a correlation matrix (Figure 1). A correlation matrix is a statistical tool used in ML to analyse the relationships between variables in a

dataset. In the context of fly ash slag-based geopolymer concrete compressive strength data, a correlation matrix helps to identify the strength of the relationships between different factors affecting concrete strength. The correlation matrix is a square matrix that displays the correlation coefficients between each pair of variables in a dataset. The coefficients range from −1 to +1, indicating the strength and direction of the relationship. When the coefficient is approximately 1, it denotes a high positive correlation, demonstrating that as one parameter increases, the other also tends to increase (pointing to a possible influencing factor). Conversely, a coefficient near −1 denotes a strong negative correlation; as one variable increases, the other decreases (indicating an opposing effect).

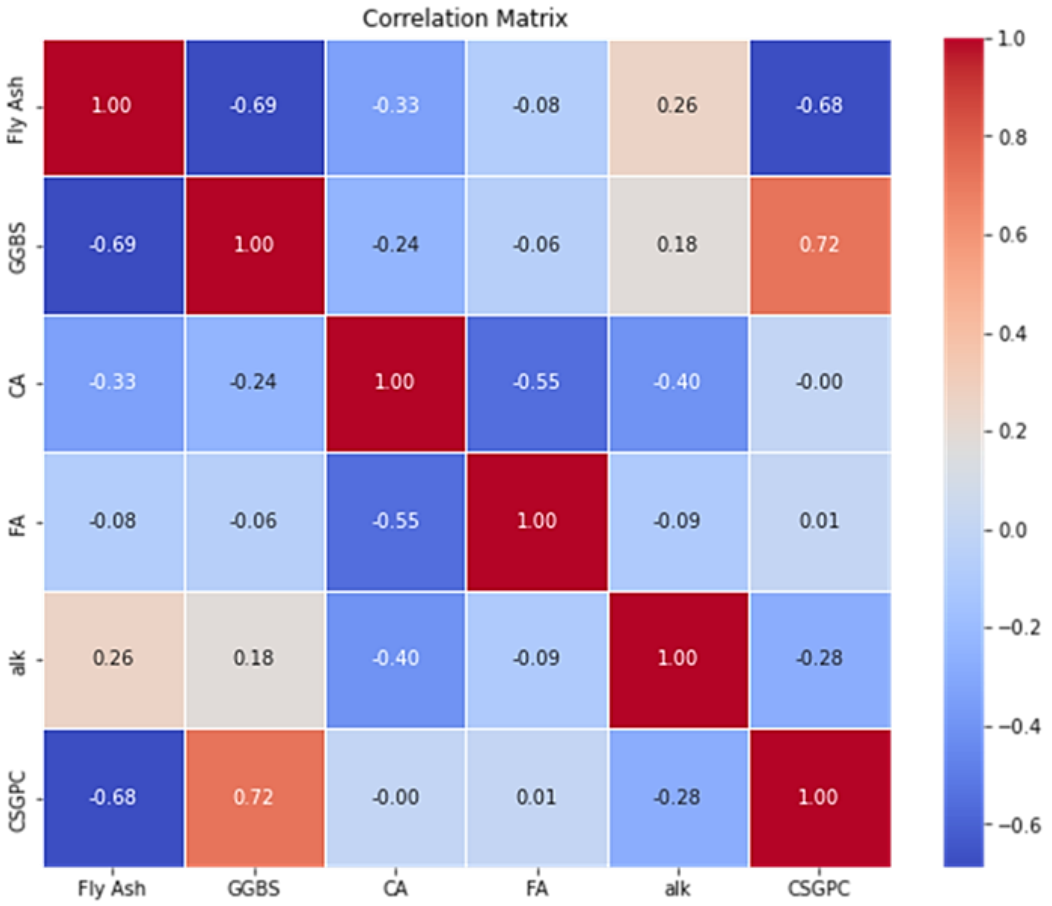

Figure 1. Correlation matrix of the input and output

2.4 Methodology of machine learning

This study analysed a dataset related to the compressive strength of fly ash and slag-based concrete. To conduct this analysis, we employed Anaconda-based Python programming, a popular platform for data analysis and ML [23] tasks. This study utilised three algorithms: RF, SVM, and LSTM. These algorithms were selected because of their effectiveness in handling complex datasets and accurately predicting the compressive strength of concrete. The section discussing different algorithms provides a detailed explanation of each algorithm. The RF is an ensemble learning method that constructs multiple decision trees during training (Figure 2) and combines their outputs to obtain more robust predictions. It is known to handle high-dimensional data and is less prone to overfitting.

Random forests are a group of regression and classification trees that are straightforward models that use binary splits of predictor variables to predict outcomes [28]. Decision trees are simple to use in practice and provide a straightforward method to predict outcomes by separating the high and low values of outcome-related predictors [29]. Despite its numerous

advantages, the decision tree approach frequently yields low accuracy for difficult datasets, such as large datasets and datasets with intricate variable relationships [30]. Several classification and regression trees were built in the RF environment utilising randomly chosen training datasets and random selections of predictor variables to model the results [31]. Each observation was predicted based on the sum of the results from each tree. As a result, random forest frequently offers more accuracy than a single decision tree model while preserving some of the advantageous features of tree models, such as the capacity to decipher the links between predictors and outcomes [32]. In the classification context, random forests regularly provide one of the greatest prediction accuracies compared with other models [33]. The flowcharts of the RF, SVM, and LSTM are shown in Figures 2, 3, and 4, respectively.

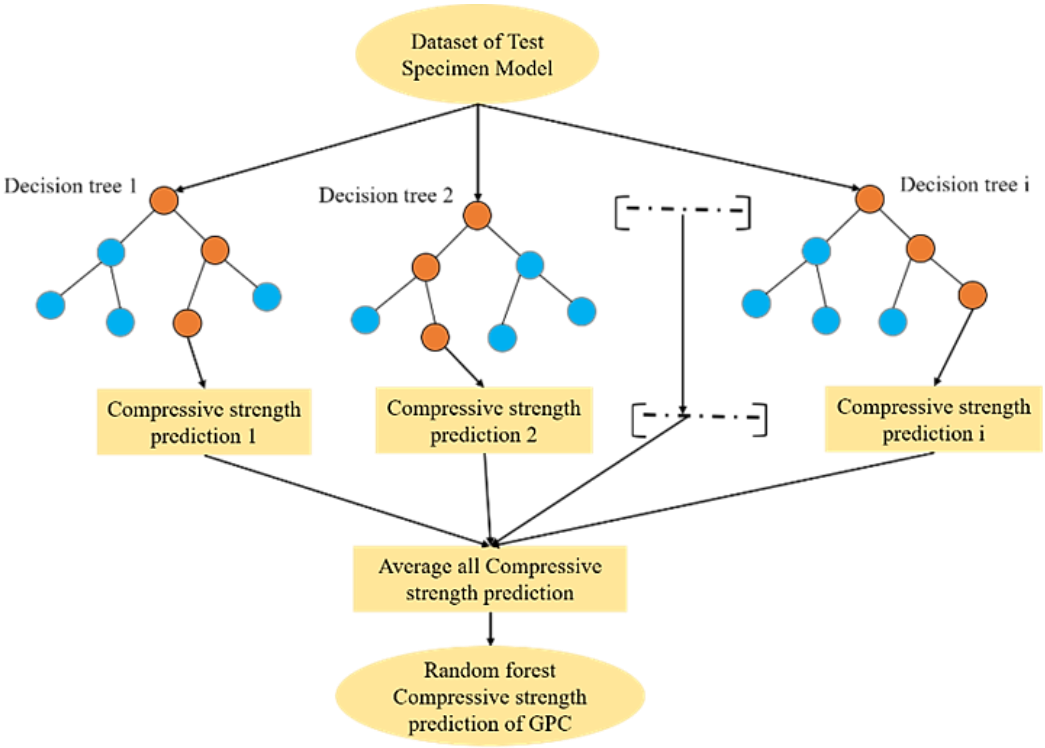

Figure 2. RF architecture

SVM is a powerful and widely used supervised learning algorithm for ML. Its primary applications include regression and classification tasks (Figure 3). The main objective of SVM is to find the best hyperplane to divide the data into distinct groups while maximising the margin between them. In the context of classification, SVM is particularly useful for dealing with data that are not linearly separable. The hyperplane represents a decision boundary that maximises the distance between the closest data points from each class, known as support vectors [34]. The greater the margin, the better the generalisation and robustness of the model to new data. SVM aims to solve a constrained optimisation problem to determine the optimal hyperplane [35]. The objective is to minimise the classification error while simultaneously maximising the margins. Optimisation involves determining the appropriate parameters for the hyperplane that best separates classes, often called weights or coefficients. An SVM was employed as an SVR for the regression tasks. It aims to fit a hyperplane such that a specified percentage of data points, known as the epsilon-insensitive zone, lies within a given margin of the predicted values. Similar to its classification counterpart, SVR seeks to find a hyperplane that optimally fits the data points, while allowing deviation tolerance.

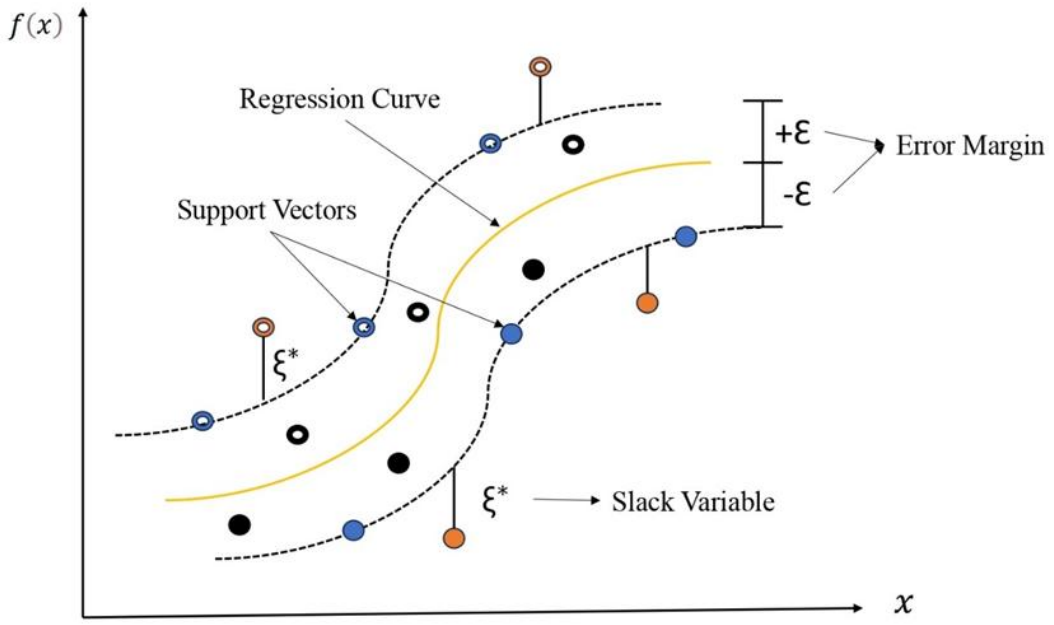

Figure 3. SVM architecture

Recurrent Neural Networks (RNNs) are a class of neural networks designed to handle sequential data by introducing a feedback loop into their architecture. LSTM is a popular type of RNN developed to address some of the limitations of traditional RNNs. LSTM networks are particularly well-suited for modelling sequential data because of their ability to capture long-range dependencies and trends in a sequence (Figure 4), making them highly appropriate for tasks involving time-series data, such as predicting concrete strength over time [36]. The main problem with traditional RNNs is the vanishing gradient problem, which arises when attempting to learn long-term dependencies in a sequence [37]. As the network backpropagates over time, the gradients can become extremely small, leading to the inability of the network to learn long-range dependencies effectively [38]. This limitation hampers the ability to capture patterns and relationships in distant sequences. LSTM networks were introduced to mitigate the vanishing gradient problem [39]. They achieved this by incorporating specialised memory cells with gating mechanisms, allowing them to store and retrieve information over extended periods [40]. The three main gates in an LSTM are the input, forget, and output gates. These gates regulate the flow of information in and out of the memory cell, enabling the network to decide which information should be retained and which should be forgotten [41].

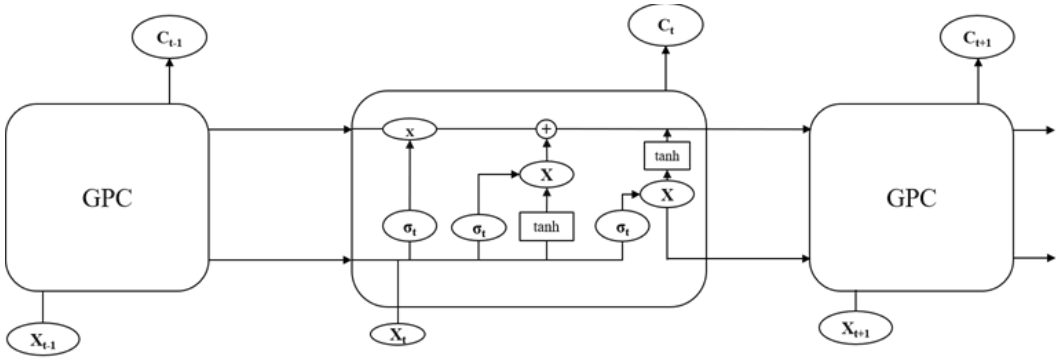

Figure 4. LSTM architecture

Table 4 presents the values of the key hyperparameters used in the prediction models to predict concrete strength. These hyperparameters are manually optimised to obtain the best

values. To optimise these hyperparameters, the values of one hyperparameter are changed to obtain the best results, whereas those of the other parameters are kept the same. This process involves a certain range of hyperparameters, beyond which there is either no impact on the accuracy of the model or a negative impact. Within the range of the hyperparameter values, the value with the best results is chosen. The next hyperparameter is optimised by maintaining the optimised value of the previous hyperparameter and the default values of the other hyperparameters. The process continues until all hyperparameters are optimised.

Table 4. Prediction models configuration

Algorithm	Parameters	Values
LSTM	number of layers	3
	number of nodes in the hidden layer and input layer	32
	epochs	200
	batch size	32
SVR	regularisation parameter (c)	1000
	gamma	0,05
	epsilon	0,01
RF	number of trees	150
	number of leaves on a tree	4
	maximum features	5
	maximum depth	10
	criterion	MSE

2.5 Model performance assessment

The coefficient of determination (R^2), root mean square error (RMSE), and mean absolute error (MAE) are standard evaluation metrics used to assess the performance of ML models, particularly in regression tasks. These metrics express how well the forecasts made by the model match the actual target values in terms of reliability and degree of fit. R^2, also known as the coefficient of determination, expresses the proportion of variability of the target, which can be explained by the independent variables (Equation 1) [42-45]. It ranges from 0 to 1, with 0 denoting that the model explains no variation, and 1 denoting a perfect fit. Lower numbers denote subpar model performance, whereas values near 1 indicate a good match.

$$R^2 = 1 - \left(\frac{\sum_{i=1}^{n} \left({CS_{GC}}_i^{P} - {CS_{GC}}_i^{a} \right)^2}{\sum_{i=1}^{n} \left({CS_{GC}}_i^{a} - \bar{CS}_{GC}^{a} \right)^2} \right);\ \bar{CS}_{GC}^{a} = \frac{1}{n} \sum_{i=1}^{n} {CS_{GC}}_i^{a} \quad (1)$$

Where ${CS_{GC}}_i^{a}$ denotes the actual value of compressive strength for the i^{th} observation; ${CS_{GC}}_i^{P}$ denotes predicted value of compressive strength for the i^{th} observation; $\overline{CS_{GC}^{a}}$ mean of actual values; and n is the number of observations.

RMSE measures the average deviation between the model predictions and target values. It computes the square root of the average squared difference between the predicted and actual values. RMSE indicates the extent to which the model predictions deviate from the true values. Lower RMSE values indicate better model performance (Equation 2) and are sensitive to outliers.

$$RMSE = \sqrt{\frac{1}{n}\left(\sum_{i=1}^{n}\left(CS_{GC_i}^{p} - CS_{GC_i}^{a}\right)^2\right)} \quad (2)$$

MAE can be used to assess how closely the model predictions match the intended values. MAE differs from RMSE in that it does not square the differences between the predicted and actual values. This means that MAE averages the absolute differences, making it a direct measure of the average error. Consequently, MAE is less sensitive to extreme values or outliers than RMSE, which squares the errors and amplifies the impact of more significant deviations. It is robust to outliers and provides a linear scale for the prediction errors (Equation 3) [42-45]. Lower MAE values indicate better model performance.

$$MAE = \frac{1}{n}\sum_{i=1}^{n}\left|CS_{GC_i}^{p} - CS_{GC_i}^{a}\right| \quad (3)$$

3 Results and discussions

3.1 Effects of different parameters on the compressive strength

The effects of the various parameters on the performance of the concrete mixture are shown in Figures 5 and 6. These figures show how altering certain factors affects the strength characteristics of the concrete. The results of these experiments provide valuable insights into the optimal composition for achieving the desired strength properties. First, the proportion of fly ash, which is a supplementary cementitious material, plays a pivotal role. As the fly ash content increased 50-70 %, a noticeable reduction in strength was observed. This indicates a diminishing effect of fly ash on concrete strength as its content increases. In contrast, the strength of the concrete increased with increasing GGBFS content, ranging 30-50 %. This emphasises the beneficial effect of GGBFS on the strength characteristics of the concrete mix. The ratio of coarse CA to FA is significant. With an increase in this ratio 1,2-1,4; a corresponding increase in strength is evident. This indicates that a slightly higher proportion of CA can positively influence the strength of concrete. However, beyond this point, the strength begins to decline when the ratio surpasses 1,4. This established an optimal CA/FA ratio of 1,4, as shown in Figure 6a). Moreover, the effect of the alkali-to-binder ratio on the compressive strength is noteworthy. As this ratio escalates 0,44-0,50, the compressive strength increases (Figure 6b). This underscores the role of alkali content in enhancing the strength of concrete. However, beyond this optimal point, the compressive strength decreases. This implies that excess alkali can harm the strength of concrete. The gathered data consequently establish an ideal alkali-to-binder ratio of 0,5 for optimal strength, as inferred from the results. These findings provide clear guidelines for achieving the optimal strength properties in concrete mixtures. The proportion of fly ash and GGBFS content exhibited opposing trends, while higher fly ash content led to reduced strength, and increased GGBFS content improved strength. The optimal ratio of CA to FA, which initially leads to strength enhancement, demonstrates the importance of striking a balance in the aggregate proportions. Similarly, the alkali-to-binder ratio shows an initial positive correlation with strength, followed by diminishing returns beyond a certain point.

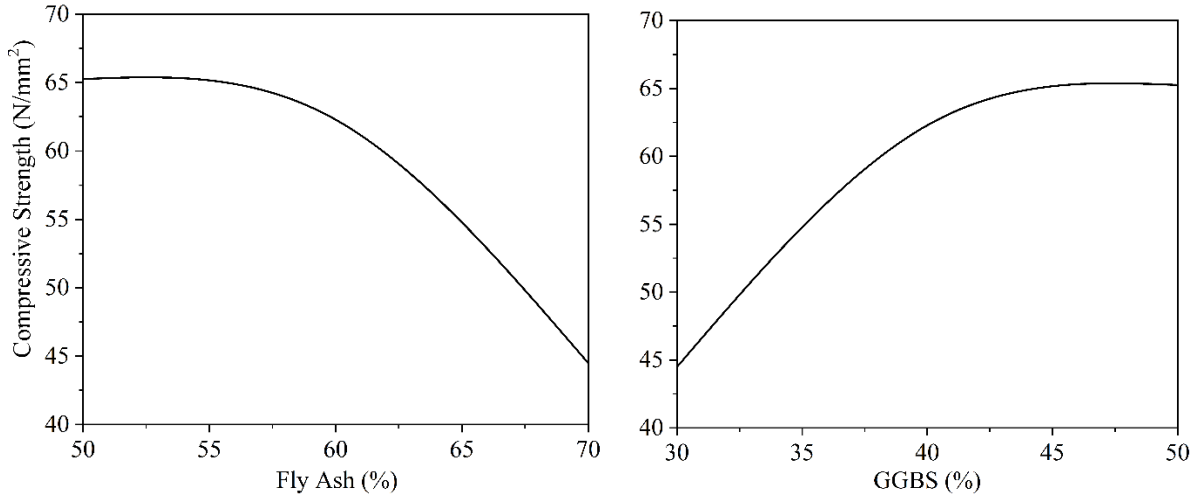

Figure 5. Compressive strength variation with the percentage of: a) fly ash; and b) GGBFS

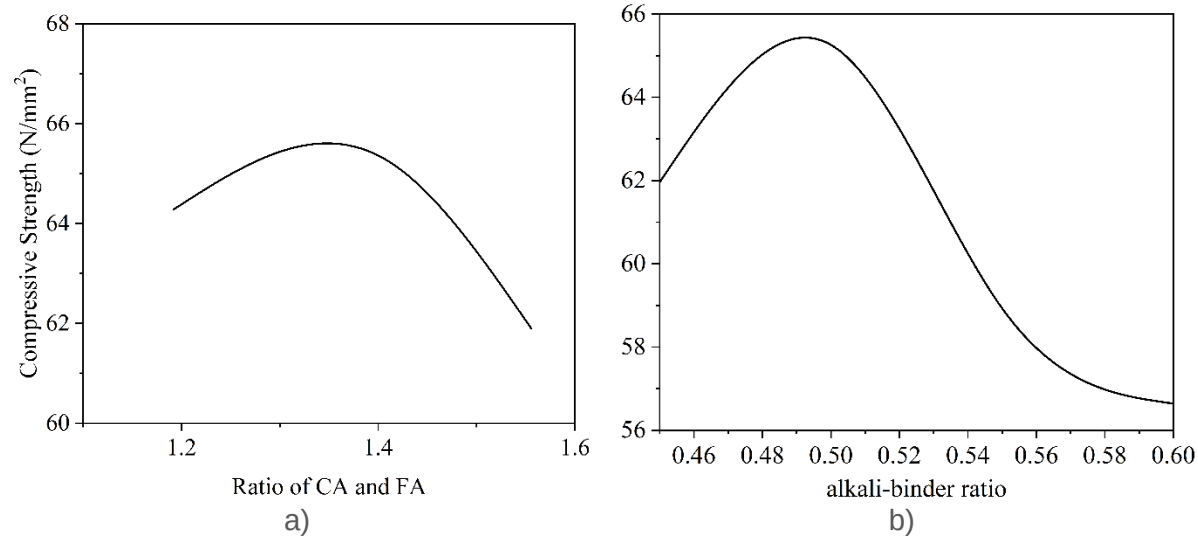

Figure 6. Compressive strength variation with the ratio of: a) CA-FA; and b) alkali-binder

3.2 Machine learning results

3.2.1 RF results

It was initially applied to these datasets to assess the RF model performance. The GPC dataset contains information on various concrete mixes, including those composed of fly ash and slag-based materials. These materials are commonly used in sustainable concrete production owing to their potential to reduce carbon emissions and enhance the durability of concrete structures. It was initially applied to these datasets to assess the RF model performance. The GPC dataset was analysed using various ML algorithms to build and evaluate the predictive models. One of the initial algorithms employed was the RF model, which was applied to the fly ash and slag-based concrete datasets, as shown in Figure 7. The performance of the RF model was evaluated using R^2. R^2 estimates the percentage of variability in the intended variable that the predictive model can correctly account for. The R^2 values for training (Figure 7a) and testing (Figure 7b) of the RF model applied to the fly ash and slag-based concrete databases were 0,89342 and 0,84398, respectively. The R^2 value of 0,89342 for training indicates that the

model explains approximately 89,34 % of the variance in the training data. In addition, the R^2 value of 0,84398 for testing indicates that the model accounts for approximately 84,40 % of the variance in the testing data. Amin et al. [46] analysed the prediction of the mechanical properties of flyash and slag-based geopolymer concrete using ML techniques and achieved an R^2 value of 0,93 with the RF model, highlighting its effectiveness in handling complex, non-linear relationships in concrete properties. Loureiro and Stefani [47] identified RF models with R^2 values of 0,868 (RMSE = 5,859) for eight predictive variables, and 0,855 (RMSE = 6,145) for six variables, demonstrating the adaptability of the model across different input configurations. Feng et al. [48] found that the RF model performed well in predicting the concrete strength. The R^2 value of oven curing for training and testing from a previous study at ambient curing was higher, and the superior performance of RF was attributed to its ability to capture complex spatial relationships in the data, making it highly effective for predicting the compressive strength of GPC [24].

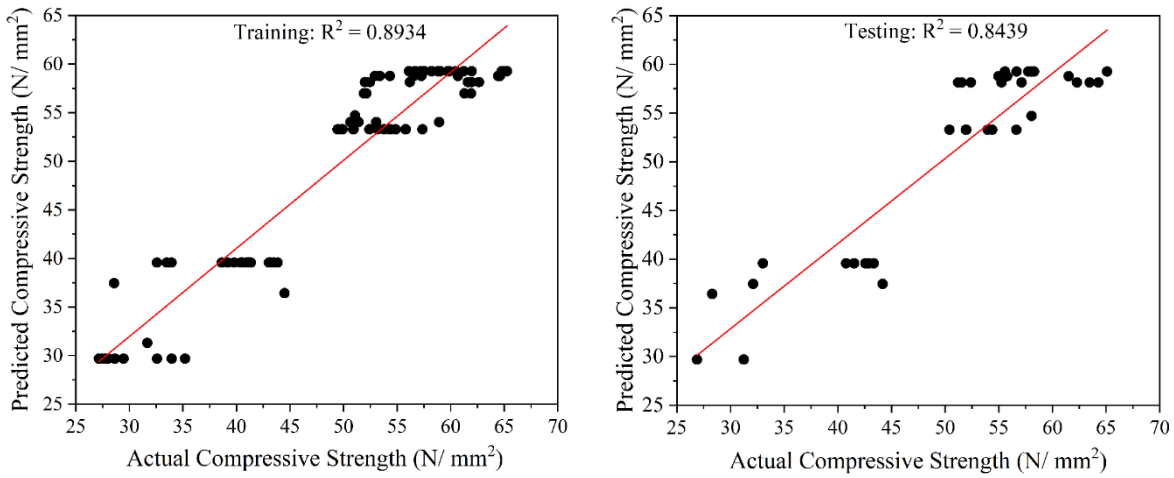

Figure 7. Relationship between predicted and actual compressive strength using RF during: a) training; b) testing

3.2.2 SVM results

The second algorithm used in this study was the SVM, which was applied to the GPC datasets (Figure 8). The core focus of this study was the application of an SVM to GPC datasets to probe its predictive probability. By utilising the R^2 metric, this study gained insight into how well the SVM model captured the inherent variability within the GPC data. Model performance was evaluated using the R^2 metric, which indicates the proportion of variance in the data explained by the model. For the training data, the R^2 value was 0,92248, indicating a good fit for the training set. The testing data showed an R^2 value of 0,86682, suggesting the ability of the model to generalise new, unseen data. Overall, the SVM model demonstrated strong predictive capabilities for the GPC datasets. This result signifies a robust fit of the model to the training set, indicating that the SVM algorithm effectively captures the underlying patterns present in the data. A high R^2 value of this magnitude suggests that the SVM model explains approximately 92,25 % of the variance observed in the training data, indicating a substantial level of accuracy in modelling GPC data complexity. The testing phase involved subjecting the SVM model to previously unseen data to assess its generalisation capability. An R^2 value of 0,86682 implies that the SVM model can account for approximately 86,68 % of the variance in the testing data, thereby demonstrating the ability of the algorithm to generalise effectively beyond the training set. This performance on the testing data implies that the SVM model does not overfit and demonstrates promising predictive capabilities, even when faced with new, unseen instances. Oven curing for training and testing had a higher R^2 value than ambient curing in earlier research, and the superior performance of SVM was ascribed to its capacity

to identify intricate spatial correlations in the data [26]. The proposed SVM model exhibited a slightly higher modelling accuracy than the linear regression technique described by Andjelkovic et al. [49] for the observed and computed strength values (R^2 = 0,83). Larger datasets can produce better prediction results, and the SVM method generally performs well in terms of generalisation and dependability [50].

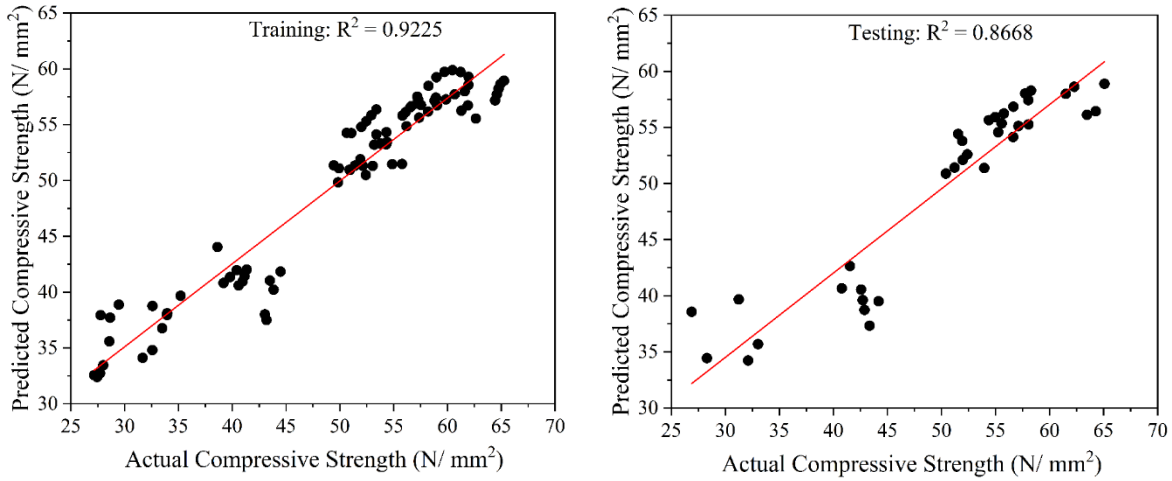

Figure 8. Relationship between predicted and actual compressive strength using SVM during: a) training; b) testing

3.2.3 LSTM results

The compressive strength of GPC is a critical parameter for assessing the performance and durability of concrete structures. The accurate prediction of this property can lead to more informed decision-making during the construction process. LSTM was used to develop a predictive model for the GPC compressive strength by leveraging its capabilities in sequence analysis. The training process involved feeding the historical data of the GPC compositions and corresponding compressive strength values into the LSTM model. The model learns the underlying patterns and correlations within the data, enabling it to make predictions based on the new inputs. The multiple memory cells and gating mechanisms of the architecture allow it to capture both short-and long-term dependencies present in the GPC data.

R^2 was employed in Figure 9 to assess the predictive capabilities of the LSTM model. The R^2 value provides insights into how well the model predictions match the actual values and ranges from 0 to 1, where 1 indicates a perfect fit. R^2 values were calculated for the training and testing phases in the study context. The R^2 value of 0,91849 obtained for the training data suggests that the LSTM model captured approximately 91,85 % of the variance in GPC compressive strength within the training dataset. This high value indicates that the model effectively learns and reproduces the underlying patterns in the training data. However, the true test of model utility is its performance on unseen data. The R2 value of 0,86942 for the testing data indicates that the LSTM model generalises well to the new and unseen GPC compositions. This value indicates that the model captured approximately 86,94 % of the variance in the compressive strength within the testing dataset. The MAE values for the RF, SVM, and LSTM were 3,4906, 2,8070, and 2,8933, respectively. The RF, SVM, and LSTM RMSE values were 4,0318, 3,9692, and 3,6921, respectively. The ability of the model to predict unseen data is a testament to its robustness and generalisation capability.

The application of LSTM to predict the GPC compressive strength underscores the potential of advanced ML techniques in the construction material domain [25]. The accurate prediction of critical properties, such as compressive strength, can enhance construction processes, improve structural safety, and optimise material usage. Although the current study

demonstrates the effectiveness of LSTM in this context, there are avenues for further exploration [50]. Fine-tuning the model architecture, exploring different data preprocessing techniques, and incorporating additional features can lead to more accurate predictions. Harun et al. [51] used LSTM to obtain greater prediction accuracy (99,55 %) than SVR (91,62 %). Sarmad [52] achieved good accuracy with R^2 = 0,98, using the LSTM model on 1030 samples to estimate the strength of concrete. Furthermore, the applicability of LSTM can extend beyond GPC to other construction materials, thereby broadening its industrial impact.

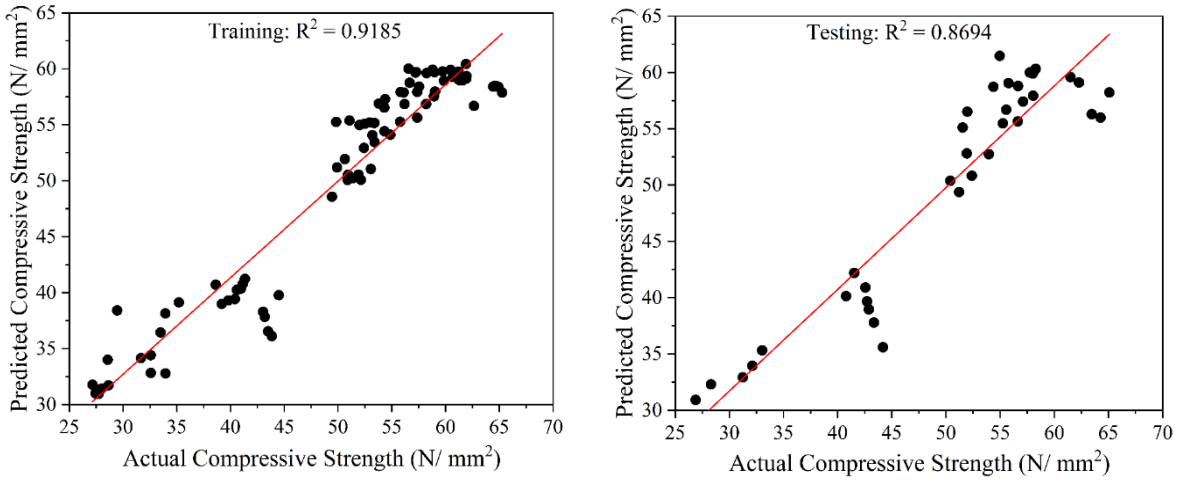

Figure 9. Relationship between predicted and actual compressive strength using LSTM during: a) training; b) testing

Hyperparameter optimisation for models, such as RF, SVM, and LSTM, involves the systematic fine-tuning of parameters to enhance model performance. For RF, key hyperparameters, such as the number of trees, tree depth, and minimum number of samples, must be tuned to achieve the best performance. In an SVM, the regularisation parameters, kernel type, gamma, and epsilon are critical. LSTM optimisation focuses on parameters such as the number of layers, units per layer, learning rate, dropout rate, and batch size. With a large number of hyperparameters and wide range of hyperparameter values, it is difficult and time consuming to manually optimise each hyperparameter. To ease the process of optimising these hyperparameters, optimisation techniques such as grid or random search, Bayesian optimisation, or hyperband, often guided by the performance of validation data to prevent overfitting, can be used [27]. All three models benefit from robust cross-validation or specific validation techniques, and the choice of the optimisation method balances exploration and exploitation to efficiently navigate the hyperparameter space.

3.2.4 SHapley Additive exPlanations (SHAP) analysis

The SHAP summary plot shows the impact of different features on the prediction of the LSTM model. Each dot represents a data point, with its position on the x-axis indicating how that feature influences the prediction (Figure 10). Positive SHAP values increase the predicted outcomes, whereas negative values decrease them. The colour gradient represents the feature value (red for high and blue for low). GGBFS has a strong negative influence when its value is low and a high positive impact when it is high, suggesting that it significantly drives the model predictions. Alkaline conditions had a smaller but consistent negative effect, whereas CA, Fly Ash, and FA had moderate influences with mixed effects. Overall, the GGBFS appeared to be the most influential feature in this analysis.

The SHAP plot helps to interpret the role of individual features in influencing predictions. Features such as GGBFS, Alkaline, CA, Fly Ash, and FA had varying levels of impact on the predictions of the LSTM model. The plot suggests that GGBFS is the most influential feature

affecting the output of the model. This implies that variations in the GGBFS value significantly change the prediction [53]. Other features, such as Alkaline and CA, exhibited a moderate influence, while Fly Ash and FA contributed to mixed effects.

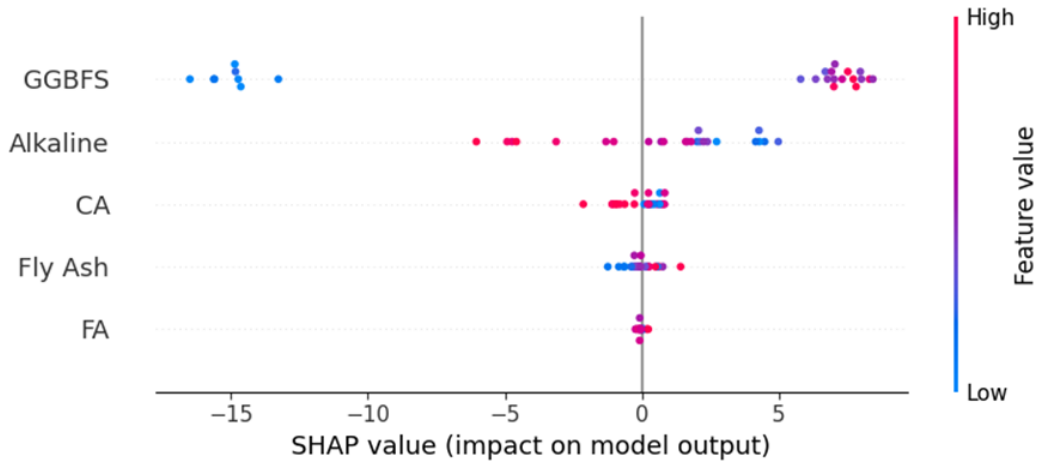

Figure 10. SHAP summary plot for feature importance in concrete strength prediction

4 Conclusions

This study was undertaken to develop an exceptional predictive model for fly ash and slag-based concrete curing in an oven under specific conditions (24 h at 65 °C). Researchers have explored the performance of three ML algorithms: RF, SVM, and LSTM. After extensive experimentation and analysis, the following conclusions were drawn:

- R^2 values for the testing models: 0,8439 for RF, 0,8668 for SVM, and 0,8694 for LSTM. The RMSE values for the RF, SVM, and LSTM were 4,0318, 3,9692, and 3,6921, respectively.
- The LSTM model achieved an R^2 value of 0,8694, indicating that it can explain approximately 86,94 % of the variance in the data, thereby demonstrating a strong and accurate fit.
- The LSTM model exhibited the lowest RMSE value of 3,6921, indicating that its predicted values are closer to the actual values than those of the RF and SVM models.
- The superiority of the LSTM model can be attributed to its unique architecture and ability to handle sequential data. LSTM is an RNN that retains the long-term dependencies and temporal patterns of an input sequence.

It is particularly suitable for modelling concrete curing processes, which inherently involve time-dependent behaviour. The findings of this study have significant implications for concrete materials and construction projects. It is important to note that the best model choice is context-dependent and may vary depending on the specific dataset and research objectives. Although LSTM proved to be the most suitable model for this study, RF and SVM may perform better in different scenarios or with diverse datasets. Additional studies and validations using various datasets are required to confirm the superiority of the LSTM model.

The limitations of this study include the reliance on a limited number of ML algorithms (RF, SVM, and LSTM) to predict the compressive strength of geopolymer concrete, which may not capture the full complexity of the underlying material behaviour. Additionally, this study focused on a specific curing technique (oven curing), potentially limiting the generalisability of the results to other curing methods or environmental conditions. Moreover, optimising the mixture composition and curing parameters significantly influences the GPC performance, which has not been fully explored, potentially leading to suboptimal results in practical applications. In

addition, the hyperparameters of ML models are optimised manually which is time consuming and does not explore all possible combinations of different hyperparameter values.

References

[1] Juenger, M. C. G.; Winnefeld, F.; Provis, J. L.; Ideker, J. H. Advances in alternative cementitious binders. *Cement and Concrete Research*, 2011, 41 (12), pp. 1232-1243. https://doi.org/10.1016/j.cemconres.2010.11.012

[2] Mehta, A.; Siddique, R. Sustainable geopolymer concrete using ground granulated blast furnace slag and rice husk ash: Strength and permeability properties. *Journal of Cleaner Production*, 2018, 205, pp. 49-57. https://doi.org/10.1016/j.jclepro.2018.08.313

[3] Wang, L. et al. Low-carbon, and low-alkalinity stabilization/solidification of high-Pb contaminated soil. *Chemical Engineering Journal*, 2018, 351, pp. 418-427. https://doi.org/10.1016/j.cej.2018.06.118

[4] Wang, L. et al.Green remediation of As and Pb contaminated soil using cement-free clay-based stabilization/solidification. *Environment International*, 2019, 126, pp. 336-345. https://doi.org/10.1016/j.envint.2019.02.057

[5] Wang, L. et al. Mechanistic insights into red mud, blast furnace slag, or metakaolin-assisted stabilization/solidification of arsenic-contaminated sediment. *Environment International*, 2019 (Part B), 105247. https://doi.org/10.1016/j.envint.2019.105247

[6] Xie, J. et al. Effects of combined usage of GGBS and fly ash on workability and mechanical properties of alkali-activated geopolymer concrete with recycled aggregate. *Composites Part B: Engineering*, 2019, 164, pp. 179-190. https://doi.org/10.1016/j.compositesb.2018.11.067

[7] Das, S.; Saha, P.; Prajna Jena, S.; Panda, P. Geopolymer concrete: Sustainable green concrete for reduced greenhouse gas emission – A review. *Materials Today: Proceedings*, 2022, 60 (1), pp. 62-71. https://doi.org/10.1016/j.matpr.2021.11.588

[8] Mallikarjuna Rao, G.; Gunneswara Rao, T. D. A quantitative method of approach in designing the mix proportions of fly ash and GGBS-based geopolymer concrete. *Australian Journal of Civil Engineering*, 2018, 16 (1), pp. 53-63. https://doi.org/10.1080/14488353.2018.1450716

[9] Oh, J. E. et al. The evolution of strength and crystalline phases for alkali-activated ground blast furnace slag and fly ash-based geopolymers. *Cement and Concrete Research*, 2010, 40, pp. 189-196. https://doi.org/10.1016/j.cemconres.2009.10.010

[10] Lee, N. K.; Lee, H. K. Setting and mechanical properties of alkali-activated fly ash/slag concrete manufactured at room temperature. *Construction and Building Materials*, 2013, 47, pp. 1201-1209. https://doi.org/10.1016/j.conbuildmat.2013.05.107

[11] Bagheri, A.; Nazari, A. Compressive strength of high strength class C fly ash-based geopolymers with reactive granulated blast furnace slag aggregates designed by Taguchi method. *Materials & Design*, 2014, 54, pp. 483-490. https://doi.org/10.1016/j.matdes.2013.07.035

[12] Farhan, N. A.; Sheikh M. N.; Hadi M. N. S. Investigation of engineering properties of normal and high strength fly ash based geopolymer and alkali-activated slag concrete compared to ordinary Portland cement concrete. *Construction and Building Materials*, 2019, 196, pp. 26-42. https://doi.org/10.1016/j.conbuildmat.2018.11.083

[13] Phoo-ngernkham, T. et al. Effects of sodium hydroxide and sodium silicate solutions on compressive and shear bond strengths of FA–GBFS geopolymer. *Construction and Building Materials*, 2015, 91, pp. 1-8. https://doi.org/10.1016/j.conbuildmat.2015.05.001

[14] Nath, P.; Sarker, P. K. Effect of GGBFS on setting, workability, and early strength properties of fly ash geopolymer concrete cured in ambient condition. *Construction and Building Materials*, 2014, 66, pp. 163-171. https://doi.org/10.1016/j.conbuildmat.2014.05.080

[15] Marjanović, N. et al. Physical–mechanical and microstructural properties of alkali-activated fly ash–blast furnace slag blends. *Ceramic International*, 2015, 41 (1 - Part B), pp. 1421-1435. https://doi.org/10.1016/j.ceramint.2014.09.075

[16] Cho, Y.-K. et al. Effect of Na2O content, SiO2/Na2O molar ratio, and curing conditions on the compressive strength of FA-based geopolymer. *Construction and Building Materials*, 2017, 145, pp. 253-260. https://doi.org/10.1016/j.conbuildmat.2017.04.004

[17] Xu, H.; Van Deventer, J. S. J. The geopolymerisation of alumino-silicate minerals. *International Journal of Mineral Processing*, 2000, 59 (3), pp. 247-266. https://doi.org/10.1016/S0301-7516(99)00074-5

[18] Bakharev, T. Geopolymeric materials prepared using Class F fly ash and elevated temperature curing. *Cement and Concrete Research*, 2005, 35 (6), pp. 1224-1232. https://doi.org/10.1016/j.cemconres.2004.06.031

[19] Papa, E. et al. Zeolite-geopolymer composite materials: Production and characterization. *Journal of Cleaner Production*, 2018, 171, pp. 76-84. https://doi.org/10.1016/j.jclepro.2017.09.270

[20] Mallikarjuna Rao, G.; Gunneswara Rao, T. D. Final Setting Time and Compressive Strength of Fly Ash and GGBS-Based Geopolymer Paste and Mortar. *Arabian Journal for Science and Engineering*, 2015, 40, pp. 3067-3074. https://doi.org/10.1007/s13369-015-1757-z

[21] Rattanasak, U.; Chindaprasirt, P. Influence of NaOH solution on the synthesis of fly ash geopolymer. *Minerals Engineering*, 2009, 22 (12), pp. 1073-1078. https://doi.org/10.1016/j.mineng.2009.03.022

[22] Albitar, M.; Mohamed Ali, M. S.; Visintin, P.; Drechsler, M. Durability evaluation of geopolymer and conventional concretes. *Construction and Building Materials*, 2017, 136, pp. 374-385. https://doi.org/10.1016/j.conbuildmat.2017.01.056

[23] Bureau of Indian Standards. IS 383. *Specification for coarse and fine aggregates from natural sources for concrete*. New Delhi: IS; 1970.

[24] Arunvivek, G. K. et al. Compressive strength modelling of cenosphere and copper slag-based geopolymer concrete using deep learning model. *Scientific Reports*, 2025, 15 (1), 27849. https://doi.org/10.1038/s41598-025-13176-z

[25] Paswan, R. K.; Kumar, P.; Kumar, V.; Sembeta, R. Y. Mechanical properties of alkali activated slag binder based concrete at elevated temperatures. *Discover Sustainability*, 2025, 6 (1), 744. https://doi.org/10.1007/s43621-025-01542-w

[26] Jiao, H. et al. A novel approach in forecasting compressive strength of concrete with carbon nanotubes as nanomaterials. *Materials Today: Communications*, 2023, 35, 106335. https://doi.org/10.1016/j.mtcomm.2023.106335

[27] Gers, F. A.; Schmidhuber, J.; Cummins, F. Learning to forget: Continual prediction with LSTM. *Neural Computation*, 2000, 12 (10), pp. 2451-2471. https://doi.org/10.1162/089976600300015015

[28] Breiman, L. Random Forests. *Machine Learning*, 2001, 45, pp. 5-32. https://doi.org/10.1023/A:1010933404324

[29] Loh, W.-Y. Fifty years of classification and regression trees. *International Statistical Review*, 2014, 82 (3), pp. 329-348. https://doi.org/10.1111/insr.12016

[30] Hastie, T.; Tibshirani, R.; Friedman, J.; Franklin, J. The elements of statistical learning: data mining, inference and prediction. *The Mathematical Intelligencer*, 2005, 27 (2), pp. 83-85. https://doi.org/10.1371/journal.pone.0123524

[31] Ho, T. K. The random subspace method for constructing decision forests. *IEEE Transactions on Pattern Analysis and Machine Intelligence*, 1998, 20 (8), pp. 832-844. https://doi.org/10.1109/34.709601

[32] Cutler, D. R. et al. Random forests for classification in ecology. *Ecology*, 2007, 88 (11), pp. 2783-2792. https://doi.org/10.1890/07-0539.1

[33] Caruana, R.; Niculescu-Mizil, A. An empirical comparison of supervised learning algorithms. In: *Proceedings of the 23rd International Conference on Machine Learning*.

June 25-29, 2006, Association for Computing Machinery, United States; 2006, pp. 161-168. https://doi.org/10.1145/1143844.1143865

[34] Kumar, P.; Sharma, S.; Pratap, B. Prediction of compressive strength of geopolymer fiber reinforced concrete using machine learning. *Civil Engineering Infrastructures Journal (CEIJ)*, 2024, 58 (1), pp. 173-182. https://doi.org/10.22059/ceij.2024.364871.1956

[35] Sharma, S.; Kumar, A.; Bano, S.; Kumar, P. Soft computing techniques for analysing the mechanical properties of eggshell powder-based concrete. *Advances in Civil and Architectural Engineering*, 2024, 15 (28), pp. 119-132. https://doi.org/10.13167/2024.28.9

[36] Graves, A. Generating sequences with recurrent neural networks. *arXiv preprint*, arXiv:1308.0850, 2013. Accessed: November 20, 2025. Available at: https://arxiv.org/abs/1308.0850

[37] Bengio, Y.; Simard, P.; Frasconi, P. Learning long-term dependencies with gradient descent is difficult. *IEEE Transactions on Neural Networks*, 1994, 5 (2), pp. 157-166. https://doi.org/10.1109/72.279181

[38] Pascanu, R.; Mikolov, T.; Bengio, Y. On the difficulty of training recurrent neural networks. *arXiv preprint*, arXiv: 1211.5063, 2012. Accessed: November 20, 2025. Available at: https://arxiv.org/abs/1211.5063

[39] Hochreiter, S.; Schmidhuber, J. Long short-term memory. *Neural Computation*, 1997, 9 (8), pp. 1735-1780. https://doi.org/10.1162/neco.1997.9.8.1735

[40] Graves, A.; Mohamed, A. R.; Hinton, G. Speech recognition with deep recurrent neural networks. In: *2013 IEEE International Conference on Acoustics, Speech and Signal Processing – Proceedings*. May 26-31, 2013, Vancouver, Canada, The Institute of Electrical and Electronics Engineers, Inc.; 2013, pp. 6645-6649. https://doi.org/10.1109/ICASSP.2013.6638947

[41] Greff, K. et al. LSTM: A search space odyssey. *IEEE Transactions on Neural Networks and Learning Systems*, 2017, 28 (10), pp. 2222-2232. https://doi.org/10.1109/TNNLS.2016.2582924

[42] Nguyen, H.; Vu, T.; Vo, T. P.; Thai, H.-T. Efficient machine learning models for prediction of concrete strengths. *Construction and Building Materials*, 2021, 266 (Part B), 120950. https://doi.org/10.1016/j.conbuildmat.2020.120950

[43] Paswan, R. K.; Gogineni, A.; Sharma, S.; Kumar, P. Predicting split tensile strength in Portland and geopolymer concretes using machine learning algorithms: a comparative study. *Journal of Building Pathology and Rehabilitation*, 2024, 9 (2), 129. https://doi.org/10.1007/s41024-024-00485-5

[44] Kumar, P.; Gogineni, A.; Kumar, A.; Modi, P. A comparative analysis of machine learning algorithms for predicting fundamental periods in reinforced concrete frame buildings. *Iranian Journal of Science and Technology, Transactions of Civil Engineering*, 2025, 49, pp. 2257-2276. https://doi.org/10.1007/s40996-024-01560-0

[45] Kumar, P. et al. Thermal performance prediction for alkali-activated concrete using GGBFS, NaOH, and sodium silicate. *Civil Engineering Infrastructures Journal*, 2024, In Press. https://doi.org/10.22059/ceij.2024.369661.1996

[46] Amin, M. N. et al. Prediction of mechanical properties of fly-ash/slag-based geopolymer concrete using ensemble and non-ensemble machine-learning techniques. *Materials*, 2022, 15 (10), 3478. https://doi.org/10.3390/ma15103478

[47] Loureiro, A. A. B.; Stefani, R. Comparing the performance of machine learning models for predicting the compressive strength of concrete. *Discover Civil Engineering*, 2024, 1, 19. https://doi.org/10.1007/s44290-024-00022-w

[48] Feng, D.-C. et al. Implementing ensemble learning methods to predict the shear strength of RC deep beams with/without web reinforcements. *Engineering Structures*, 2020, 235, 111979. https://doi.org/10.1016/j.engstruct.2021.111979

[49] Andjelkovic, V.; Pavlovic, N.; Lazarevic, Z.; Radovanovic, S. Modelling of shear strength of rockfills used for the construction of rockfill dams. *Soils and Foundations*, 2018, 58 (4), pp. 881-893. https://doi.org/10.1016/j.sandf.2018.04.002

[50] Chen, H. et al. Compressive strength prediction of high-strength concrete using long short-term memory and machine learning algorithms. *Buildings*, 2022, 12 (3), 302. https://doi.org/10.3390/buildings12030302

[51] Tanyildizi, H. Predicting the geopolymerization process of fly ash-based geopolymer using deep long short-term memory and machine learning. *Cement and Concrete Composites*, 2021, 123, 104177. https://doi.org/10.1016/j.cemconcomp.2021.104177

[52] Latif, S. D. Concrete compressive strength prediction modeling utilizing deep learning long short-term memory algorithm for a sustainable environment. *Environmental Science and Pollution Research*, 2021, 28, pp. 30294-30302. https://doi.org/10.1007/s11356-021-12877-y

[53] Wang, Z. et al. Optimizing machine learning techniques and SHapley Additive exPlanations (SHAP) analysis for the compressive property of self-compacting concrete. *Materials Today: Communications*, 2024, 39, 108804. https://doi.org/10.1016/j.mtcomm.2024.108804